



ELSEVIER

Available online at www.sciencedirect.com

Earth and Planetary Science Letters 268 (2008) 41–51

 EPSL

www.elsevier.com/locate/epsl

Subsidence of normal oceanic lithosphere, apparent thermal expansivity, and seafloor flattening

Tomoko Korenaga, Jun Korenaga *

Department of Geology and Geophysics, Yale University, P.O. Box 208109, New Haven, CT 06520-8109, USA

Received 20 November 2006; received in revised form 5 September 2007; accepted 24 December 2007

Available online 18 January 2008

Editor: C.P. Jaupart

Abstract

Seafloor topography has been a key observational constraint on the thermal evolution of oceanic lithosphere, which is the top boundary layer of convection in Earth's mantle. At least for the first ~70 Myr, the age progression of seafloor depth is known to follow the prediction of half-space cooling, and the subsidence rate is commonly believed to be ~350 m Ma^{-1/2}. Here we show that, based on a new statistical analysis of global bathymetry, the average subsidence rate of normal oceanic lithosphere is likely to be ~320 m Ma^{-1/2}, i.e., ~10% lower than the conventional value. We define the 'normal' seafloor as regions uncorrelated with anomalous crust such as hotspots and oceanic plateaus, but the lower subsidence rate appears to be a stable estimate, not depending on how exactly we define the normal seafloor. This low subsidence rate can still be explained by half-space cooling with realistic mantle properties, if the effective thermal expansivity of a viscoelastic mantle is taken into account. In light of a revised model of half-space cooling, the normal seafloor unperturbed by the emplacement of anomalous crust exists for all ages, and the so-called seafloor flattening seems to be mostly caused by hotspots and oceanic plateaus.

© 2008 Elsevier B.V. All rights reserved.

Keywords: mantle convection; depth anomalies; thermal cracking

1. Introduction

Hot suboceanic mantle beneath mid-ocean ridges is gradually cooled from above as it moves laterally by plate motion. Because the thermal diffusivity of mantle rocks is ~10⁻⁶ m² s⁻¹ and seafloor is younger than 200 Ma, the vertical extent of thermal diffusion is on the order of 100 km. As this length scale is considerably shorter than the depth extent of Earth's mantle (~3000 km), it is reasonable to expect that the surface cooling of suboceanic mantle can be approximated as the cooling of a semi-infinite medium or half-space cooling, and indeed, the observed age–depth relationship of seafloor supports this simple cooling model, at least for seafloor younger than ~70 Ma. The interpretation of the age–depth relationship for older seafloor has been controversial (see Section 4.2 for discussion), and our primary analysis will focus on the

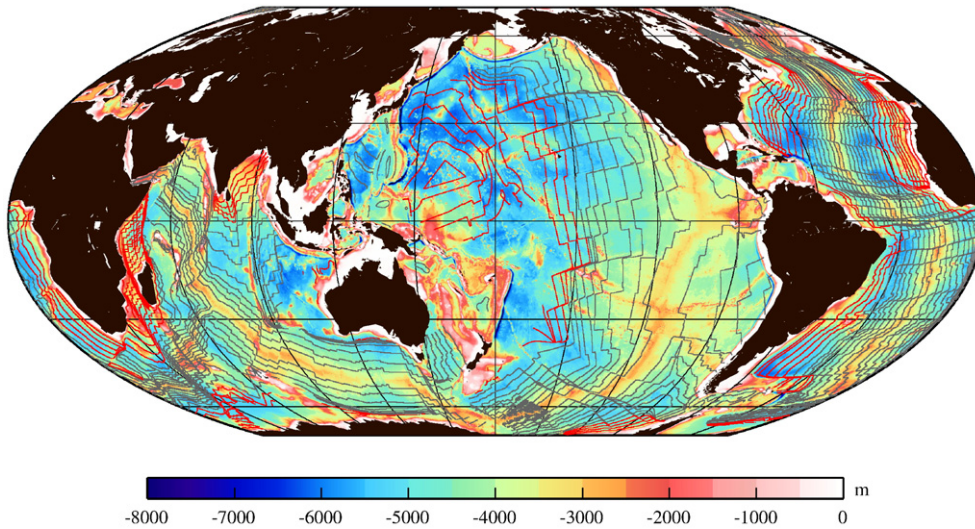
characteristics of seafloor younger than 70 Ma. This part of seafloor is commonly regarded to be well understood, with the subsidence rate of ~350 m Ma^{-1/2} (Parsons and Sclater, 1977; Stein and Stein, 1992; Carlson and Johnson, 1994; Smith and Sandwell, 1997), but as shown in this paper, the conventional understanding does not seem to properly represent the global characteristics of young seafloor. Along with heat flow, seafloor depth (Fig. 1a) has been a key observational constraint on the thermal evolution of oceanic lithosphere (Parsons and Sclater, 1977; Stein and Stein, 1992), so it is important to establish a representation that is more faithful to actual data. A better understanding of the younger part of seafloor has an important bearing on the interpretation of the older part as well.

The main purpose of this paper is to construct a statistical description for the subsidence of seafloor younger than 70 Ma, and in particular, normal seafloor unperturbed by the emplacement of anomalous crust such as hotspot islands and oceanic plateaus. This task is not so straightforward because there is no consensus in the literature on how to define the 'normal' seafloor. In this paper, therefore, we introduce a new statistical

* Corresponding author. Tel.: +1 203 432 7381; fax: +1 203 432 3134.

E-mail addresses: tomoko.korenaga@yale.edu (T. Korenaga), jun.korenaga@yale.edu (J. Korenaga).

(a) Bathymetry with isochrons



(b) Residual Bathymetry

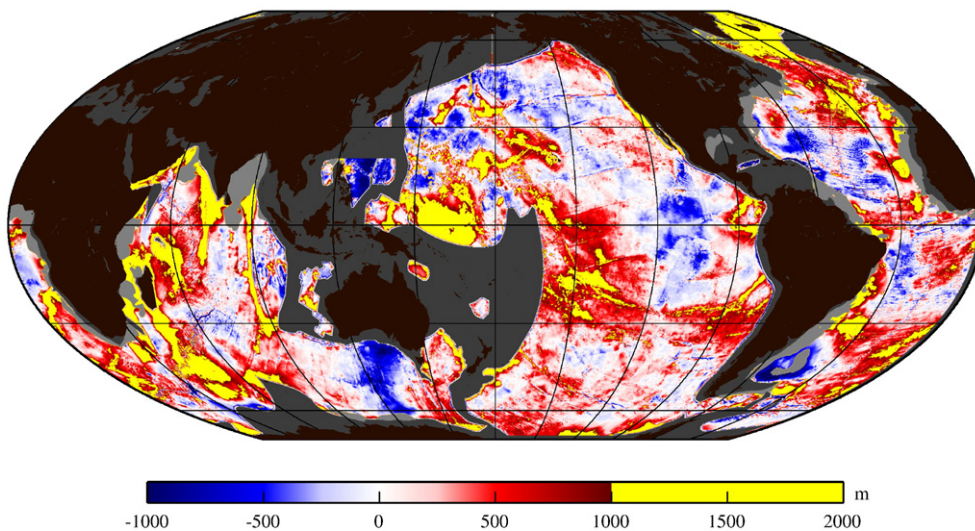


Fig. 1. (a) Predicted bathymetry of Smith and Sandwell (1997) with isochrons for seafloor age (Müller et al., 1997) (red contours for $t \geq 80$ Ma). (b) Residual bathymetry with respect to the plate model of Stein and Stein (1992). The effect of sediment loading was corrected by applying the empirical relation of Schroeder (1984) to the global sediment thickness database (Divins, 2006), and we also exclude regions with sediments thicker than 2 km (denoted by light gray) because sediment correction becomes inaccurate. Dark gray areas denote where either age or sediment data are unavailable. Yellow shading signifies regions with residual depth greater than 1 km, which correspond well to the distribution of hotspot chains and oceanic plateaus. (For interpretation of the references to color in this figure legend, the reader is referred to the web version of this article).

approach based solely on the seafloor topography. As will be shown, a simple but hitherto overlooked spatial correlation allows us to delineate the extent of unperturbed seafloor. By combining with the bootstrap resampling method, then, we will construct a statistical representation for the thermal subsidence of the normal seafloor. Though some degrees of nonuniqueness still remain, we will show that the subsidence of the normal seafloor is only marginally comparable with the conventional wisdom; our analysis indicates that the global subsidence rate is more likely to be $\sim 320 \text{ m Ma}^{-1/2}$. Finally, we will discuss the implications of this revised rate for the evolution of oceanic lithosphere, including its behavior at ages older than 70 Ma.

2. Statistical representation of age–depth relationship

We first stress that, as a number of seismic studies demonstrate (White et al., 1992), there clearly exist anomalous crustal regions in various places of ocean basins, and we must exclude them a priori if our goal is to understand the evolution of normal oceanic lithosphere. Due to isostasy, regions with anomalously thick crust usually appear as pronounced topographic highs. Fig. 1b shows residual bathymetry using the plate model of Stein and Stein (1992) as a reference, and it can be seen that regions with residual depth anomaly greater than 1 km (shown by yellow) are mostly associated with known hotspots and plateaus (Coffin and Eldholm,

1994). This motivated us to identify the anomalous crustal regions using residual bathymetry; crustal seismic experiments are far from covering all ocean basins. In order to eliminate isolated seamounts and limit ourselves to well-known hotspot chains and oceanic plateaus, we applied a Gaussian filter of 150 km diameter to residual bathymetry and define regions still characterized by >1 km anomaly as “anomalous crust”.

The age–depth relationship for all seafloor (with known age) excluding the anomalous crust is given in Fig. 2a. Half-space cooling predicts that depth is linearly proportional to \sqrt{t} (Turcotte and Schubert, 1982), where t is the age of seafloor, and it is reasonable to assume this cooling model for seafloor younger than ~70 Ma. The older seafloor tends to deviate to shallower depths, and this phenomenon is often called as seafloor flattening. In any

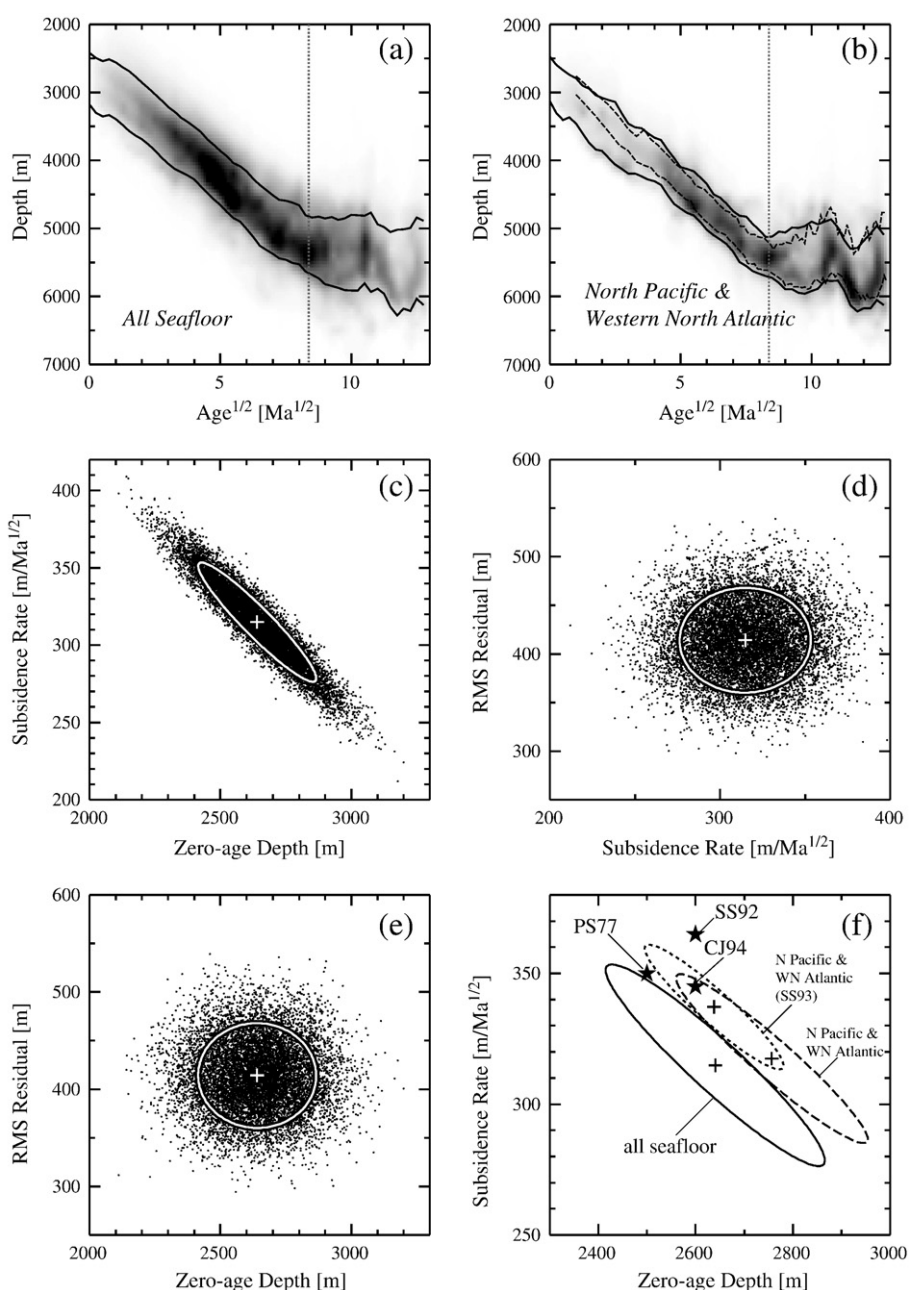


Fig. 2. (a) Age–depth relation for all seafloor with known age and sediment thickness but excluding the anomalous crust as defined in the text. Regions with sediments thicker than 2 km (light gray region in Fig. 1b) are also excluded because of unreliable sediment correction. Solid curves denote the depth interval corresponding to one standard deviation, and dotted line is drawn at 70 Ma. (b) Same as (a) but for the North Pacific (140°E–100°W and 0°–60°N) and the western North Atlantic (80°W–40°W and 15°N–45°N). These are the same regions considered by Stein and Stein (1992, 1993). Dashed curves are the depth interval reported by Stein and Stein (1993) on the basis of older age–depth data (Sclater and Wixon, 1986; Renkin and Sclater, 1988). (c) Joint distribution of zero-age depth and subsidence rate, based on the bootstrap resampling from the age–depth relation of (a). The error ellipse is drawn for the 68% confidence zone. (d) Distribution of RMS residual of linear regression as a function of the subsidence rate. (e) Same as (d) but as a function of the zero-age depth. (f) Comparison of the estimated subsidence parameters with previous studies (PS77, Parsons and Sclater, 1977, SS92, Stein and Stein, 1992, and CJ94, Carlson and Johnson, 1994). Error ellipses (68% confidence zone) are shown for the global case (solid, based on (a)) and two regional cases (dashed, based on (b), and dotted, based on Stein and Stein (1993)).

case, the following statistical model may be sufficient for seafloor younger than 70 Ma:

$$d(t) = d_0 + b\sqrt{t} + \varepsilon, \quad (1)$$

where $d(t)$ is the seafloor depth at the age of t , d_0 is the zero-age depth, b is the subsidence rate, and ε denotes the prediction error. Note that d_0 , b , and ε are all random variables. The zero-age depth and subsidence rate can only be known with some uncertainty. The error term ε is essential because half-space cooling predicts only one depth for a given age and by itself cannot account for the observed depth distribution, which is on the order of ± 400 m. The thickness of normal oceanic crust has a standard deviation of ~ 1 km (White et al., 1992), which alone results in ~ 200 m depth variation, and the rest of variability may be caused by dynamic topography due to mantle convection of various spatial scales (Kido and Seno, 1994). Errors in seafloor age, predicted bathymetry, and sediment correction can also contribute to prediction error. We assume that ε follows a Gaussian distribution with zero mean and (age-independent) standard deviation, σ_ε .

In order to estimate the statistical distribution of these random variables, we employ the boot-strap resampling method (Efron, 1982). Using the actual depth distribution as a proxy to the probability distribution, we randomly sample depth data uniformly from 0 Ma to 70 Ma with 1 Myr interval. Each bootstrap ensemble thus has 71 depth data, and we repeat linear regression for 10^4 ensembles. The joint probability density function of d_0 and b can be estimated from the distribution of intercept and slope (Fig. 2c), whereas σ_ε may be estimated from the root-mean-square (RMS) residual (Fig. 2d,e). The zero-age depth and the subsidence rate are negatively correlated (with the correlation coefficient of -0.94), with $d_0 = 2630 \pm 150$ m and $b = 315 \pm 26$ m Ma $^{-1/2}$. These uncertainties are one standard deviation (i.e., 68% confidence interval) for the case of considering these two parameters separately, and the 68% confidence region on them jointly (as depicted by an ellipse in Fig. 2c) exceeds these marginal bounds. The standard deviation of prediction error is estimated to be ~ 410 m.

This resampling method has two advantages. First, seafloor depth is sampled uniformly from the age interval of 0–70 Ma. The area-age distribution of the actual seafloor is known to be biased to younger seafloor, i.e., there is less seafloor at older ages, and random subduction irrespective of seafloor age provides a simple explanation for this distribution (Parsons, 1982). If we use the all depth data directly, therefore, regression would be biased to younger seafloor data. The uniform age sampling can avoid this bias. Second, the sampling is done globally, not regionally, and this global sampling is essential to extract the average subsidence rate and its uncertainty from the global data. Alternatively, one may divide the seafloor into a number of tectonic corridors (with common ancestral mid-ocean ridge segments) and study their subsidence rates separately (Marty and Cazenave, 1989). These regional subsidence rates are known to vary widely from place to place (~ 150 m Ma $^{-1/2}$ to ~ 400 m Ma $^{-1/2}$), but these regional rates and their variability are of little use in constraining the half-space cooling model. For example, when Marty and Cazenave (1989) interpreted the

subsidence rate of a particular tectonic corridor in terms of half-space cooling, it was assumed that mantle temperature beneath its ancestral segment remains constant for the entire evolution of this corridor, but this assumption is hard to justify. At present, mantle temperature beneath mid-ocean ridges varies probably by ± 50 – 100 K (Klein and Langmuir, 1987; Herzberg et al., 2007), so we can also expect temporal variations with a similar magnitude beneath a particular ridge segment. A tectonic corridor characterized by a low subsidence rate, for example, may be caused by a gradual transition from a hotter ridge segment in the past to a colder one in the present. Note that it is impossible to distinguish between spatial and temporal variations in the present-day seafloor data because temporal variations are mapped into spatial variations. Random re-sampling from the global data can properly map these regional fluctuations into the uncertainty of the average subsidence behavior without being trapped by them.

Though our estimate of the global subsidence rate is characterized by a relatively large uncertainty (~ 20 – 40 m Ma $^{-1/2}$), its mean value (~ 315 m Ma $^{-1/2}$) is still notably lower than the conventional rate of ~ 350 m Ma $^{-1/2}$, and this discrepancy demands an explanation. First of all, we note that the classic studies of Parsons and Sclater (1977) and Stein and Stein (1992) are not based on global data; their analyses are based on age–depth data from the North Pacific and the western North Atlantic. The age–depth data for these regions are plotted in Fig. 2b, which exhibit a somewhat more restricted distribution. We repeated the bootstrap resampling with this distribution, and obtained that $d_0 = 2760 \pm 130$ m and $b = 317 \pm 21$ m Ma $^{-1/2}$ with the correlation coefficient of -0.94 (Fig. 2f). Thus, the low subsidence rate does not seem to be simply due to regional variations. A closer look indicates that the different vintages of age–depth data may be a source of discrepancy. The analysis of Stein and Stein (1992, 1993) (and also of Carlson and Johnson (1994)) is based on older age–depth data (Sclater and Wixon (1986) for the western North Atlantic and Renkin and Sclater (1988) for the North Pacific), and Fig. 2 shows that these data sets have too narrow depth distribution for seafloor younger than ~ 10 Ma. The bootstrap resampling with this distribution results in $d_0 = 2640 \pm 95$ m and $b = 337 \pm 16$ m Ma $^{-1/2}$ with the correlation coefficient of -0.94 , which is more comparable with the conventional estimates (Fig. 2f). Fig. 2b suggests that the subsidence rate of ~ 350 m Ma $^{-1/2}$ would be consistent with this older and regional age–depth data, which is slightly biased to shallow depths at young ages, but the global data do not support such age–depth distribution (Fig. 2a).

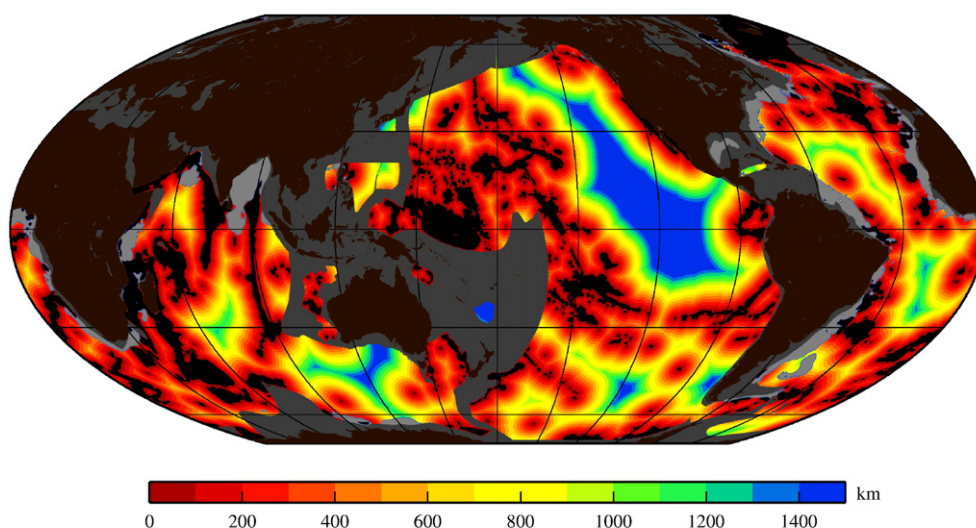
However, one may wonder whether the global age–depth distribution (Fig. 2a) may be too broad or blurred, which may result in the low subsidence rate. This criticism may be adequate because we excluded only the most prominent topographic highs (defined as the anomalous crust), and this filtering does not guarantee that the rest of seafloor can be considered as ‘normal’ (although we should note that the age–depth distribution of Stein and Stein (1993), which was used by Stein and Stein (1992) and Carlson and Johnson (1994), does not involve any filtering effort). In fact, how to define the normal seafloor has been a tricky subject. In the next section, therefore, we first discuss this issue and then revisit the age–depth relationship.

3. New age–depth relationship for the normal seafloor

How to define the normal seafloor, i.e., the unperturbed seafloor not affected by hotspots and plateaus, has been ambiguous in the literature. Some previous studies (Parsons and Sclater, 1977; Renkin and Sclater, 1988; Stein and Stein, 1992) did not even exclude such anomalous crust when estimating a reference cooling model. Schroeder (1984), on the other hand, showed that seafloor subsidence in the Pacific follows simple half-space cooling, if seafloor within 600 km from known hotspot tracks is excluded, and based on this, Davies (1988) questioned the significance of seafloor flattening. With this aggressive filtering, however, the normal seafloor is

almost nonexistent for ages greater than 80 Ma. This filtering may also be regarded as arbitrary because how far hotspots could actually influence the surrounding seafloor is not well understood. Recently, Hillier and Watts (2005) developed a filtering technique to remove bathymetric anomalies from ship track data, but their implementation appears to be a mere automation of visual inspection. In another recent study, Crosby et al. (2006) first masked out hotspot chains and plateaus by eye and then defined regions with nearly zero gravity anomalies as unperturbed seafloor. Though the use of correlation between topography and gravity may be appealing, it is not particularly suited to distinguish unperturbed regions because buoyancy perturbations to lithosphere from below are fundamentally

(a) Distance from anomalous regions



(b) Correlation between distance and residual depth

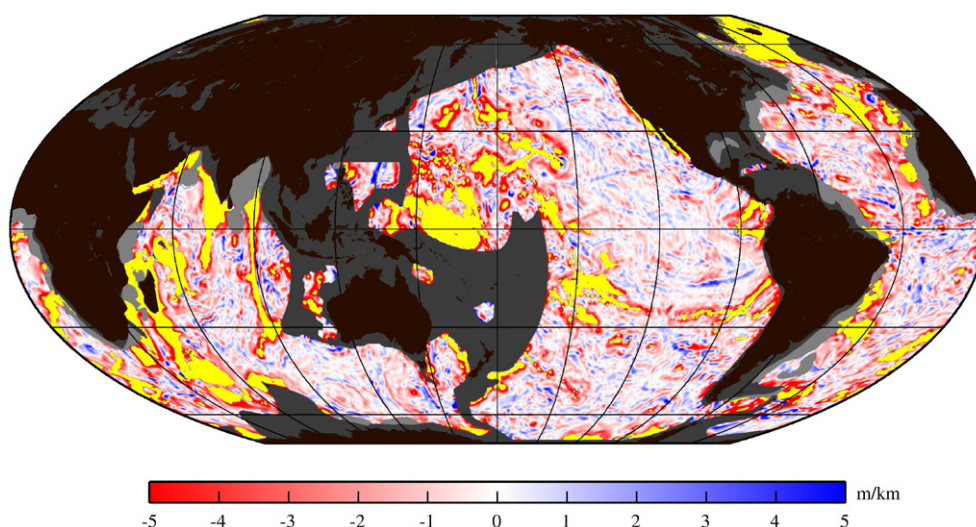


Fig. 3. (a) Distance to the nearest anomalous crust (shown in solid). (b) Correlation between residual depth and distance to the nearest anomalous crust. A search radius of 100 km is used for the calculation of spatial correlation. Negative correlation (red) implies the strong influence of anomalous crust (shown in yellow) on surrounding seafloor. The meaning of gray shadings is the same as in Fig. 1(b). (For interpretation of the references to color in this figure legend, the reader is referred to the web version of this article).

biased to be positive. To claim a region with zero gravity anomaly as unperturbed, symmetrical density perturbations are implicitly assumed, but it is unlikely. There is no cold (and thus denser-than-surrounding) plume rising in the mantle, so it is hard to imagine a mechanism to add negative buoyancy to normal lithosphere from below. What has been frustrating is that currently available geophysical data do not have sufficient resolution to map out the spatial extent of the unperturbed seafloor on the basis of subsurface structure.

We suggest that a new statistical approach, requiring only the seafloor topography, may add a fresh perspective to the continuing debate on the definition of the normal seafloor. We previously defined the anomalous crust as the regions with residual bathymetry greater than 1 km, because such regions correspond reasonably well to known hotspots and plateaus (Fig. 1b). What we also see is that remaining positive depth anomalies (red) are almost always located near anomalous crust (yellow). This indicates that the anomalous crust does not exist without affecting the surrounding seafloor, so we have to consider a part of the surrounding seafloor as perturbed by the emplacement of anomalous crust. Such spatial connection can be understood as, for example, a result of thermal and chemical buoyancy associated with mantle plumes (Ribe and Christensen, 1994; Phipps Morgan et al., 1995). In addition to creating hotspot islands by melting, a mantle plume can thermally and mechanically erode the base of the lithosphere, and a chemically buoyant depleted mantle after melt extraction may also spread beneath the lithosphere. It is thus natural to expect that the seafloor surrounding hotspot islands is affected by such sublithospheric dynamics. Unfortunately, how widely such dynamics would affect the surrounding seafloor depends on a number of poorly constrained parameters including the radius of a plume and its ascent velocity, plume temperature, the chemical composition of plume material, the degree of melting, and the viscosities of asthenosphere and depleted mantle, so theoretically predicting the radius of plume influence is difficult. Strong spatial correlation as depicted by Fig. 1b, however, suggests that

the spatial extent of perturbed seafloor may be constrained on a purely statistical ground. Note that the predicted topography of Smith and Sandwell (1997) is partly based on gravity, but because the method we will propose below do not rely on the correlation between gravity and topography, its use does not lead to any circular argument. A comparison among different versions of predicted topography indicates that its long wavelength features are robust (Calmant et al., 2002). The use of predicted topography, which is constrained by shipboard soundings, is unlikely to introduce any major bias, and it only facilitates our global analysis.

The spatial association between anomalous crust and surrounding seafloor can be quantified by calculating how residual depth anomaly changes as we move away from anomalous crust. To this end, we first need to assign a distance to the nearest anomalous crust for all points in the surrounding seafloor (we used 5 minute by 5 minute grid resolution throughout our analysis), for which we used the graph-theoretical (shortest-path) method (Moser, 1991) (Fig. 3a). Using this distance map, we then calculated correlation between distance and (unfiltered) residual depth. When the presence of anomalous crust appears to raise a part of surrounding seafloor, such perturbed seafloor should be characterized by negative correlation. That is, as we move away from the anomalous crust, residual bathymetry decreases. For each grid point in the surrounding seafloor, correlation is calculated by least-squares using all points (excluding anomalous crust) that fall in a given search radius. We have tested different search radii ranging from 50 km to 150 km, with virtually no difference in long-wavelength patterns. A case of 100 km search radius is shown in Fig. 3b. We note that, because this correlation is sensitive only to regional gradients in bathymetry, it hardly depends on a particular choice of a reference cooling model used to define residual bathymetry.

The aerial distribution of this correlation is summarized as a function of distance to the nearest anomalous crust (Fig. 4a) and as a function of residual depth (Fig. 4b). As Fig. 4a indicates, the influence of anomalous crust generally diminishes at distance of

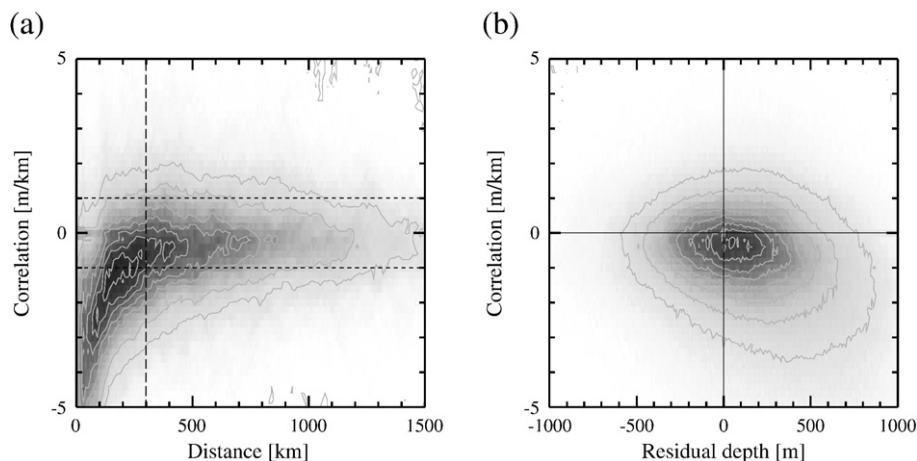


Fig. 4. (a) Areal distribution of correlation as a function of distance to the nearest anomalous crust. Darker shading denotes larger area. Our estimate for background noise level ($\pm 1 \text{ m km}^{-1}$) is denoted by dotted lines. Dashed line is drawn at the distance of 300 km, which we use in the distance criterion for the normal seafloor. (b) Same as (a) but as a function of residual depth.

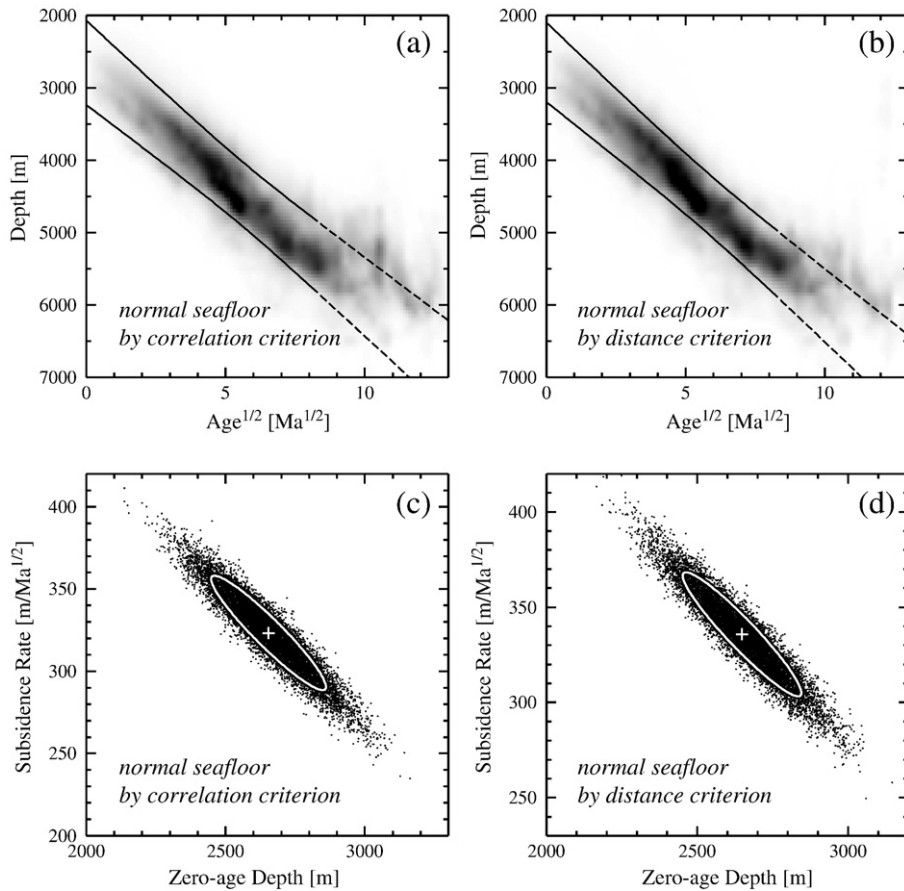


Fig. 5. (a) Age–depth relation for normal seafloor according to the correlation criterion. Curves denote the depth interval that is consistent with half-space cooling, on the basis of bootstrap resampling analysis. The uncertainty of zero-age depth and subsidence rate (corresponding to the 68% confidence zone) as well as one standard deviation of prediction error are taken into account. Dashed curves for ages greater than 70 Ma emphasize their predicted nature as only younger seafloor is used for bootstrap analysis. (b) Same as (a) but with the distance criterion. (c) Joint distribution of zero-age depth and subsidence rate, based on the bootstrap resampling from the age–depth relation of (a). The error ellipse is drawn for the 68% confidence zone. (d) Same as (c) but for the age–depth relation of (b).

~300 km, and back-ground noise level for correlation is about $\pm 1 \text{ m km}^{-1}$. Based on this observation, seafloor with correlation larger than -1 m km^{-1} may be regarded as unperturbed by the formation of anomalous crust. For comparison, we may simply choose to accept seafloor located more than 300 km away from the anomalous crust. We refer to the former as the correlation criterion and the latter as the distance criterion. The correlation criterion allows us to remove perturbed seafloor using *variable* distance to anomalous crust with some confidence. Fig. 4b shows that regions with positive residual depth are biased to have negative correlation. This confirms our visual impression for Fig. 1b, that is, positive depth anomalies are mostly found in the vicinity of anomalous crust.

The age–depth relationship for the normal seafloor is shown in Fig. 5a for the correlation criterion and in Fig. 5b for the distance criterion. As in the previous section, we use the seafloor with ages younger than 70 Ma to estimate the subsidence parameters, with the results of $d_0 = 2654 \pm 137 \text{ m}$ and $b = 323 \pm 23 \text{ m Ma}^{-1/2}$ for the former (Fig. 5c) and $d_0 = 2648 \pm 130 \text{ m}$ and $b = 336 \pm 22 \text{ m Ma}^{-1/2}$ for the latter (Fig. 5d). For both cases, the correlation coefficient is around -0.94 and the standard deviation of prediction error is ~ 350 –

380 m. Even with these aggressive filtering, therefore, the average subsidence rate still seems to be systematically lower than $350 \text{ m Ma}^{-1/2}$ (Fig. 6). We note that a similar conclusion was previously obtained by Heestand and Crough (1981) (for the North Atlantic, $b = 295 \text{ m Ma}^{-1/2}$ with the distance criterion of $> 1000 \text{ km}$) and Schroeder (1984) (for Pacific, $b = 314 \text{ m Ma}^{-1/2}$ with the distance criterion of $> 800 \text{ km}$). Though regional subsidence rates are known to exhibit substantial scatters (Marty and Cazenave, 1989) (Fig. 6), these earlier studies may cover sufficient area to approach the global average.

4. Discussion

4.1. Physical meaning of the low subsidence rate

Assuming half-space cooling with constant material properties, the subsidence rate may be expressed as (Turcotte and Schubert, 1982):

$$b = \frac{2\alpha\rho_m\Delta T\sqrt{\kappa/\pi}}{\rho_m - \rho_w}, \quad (2)$$

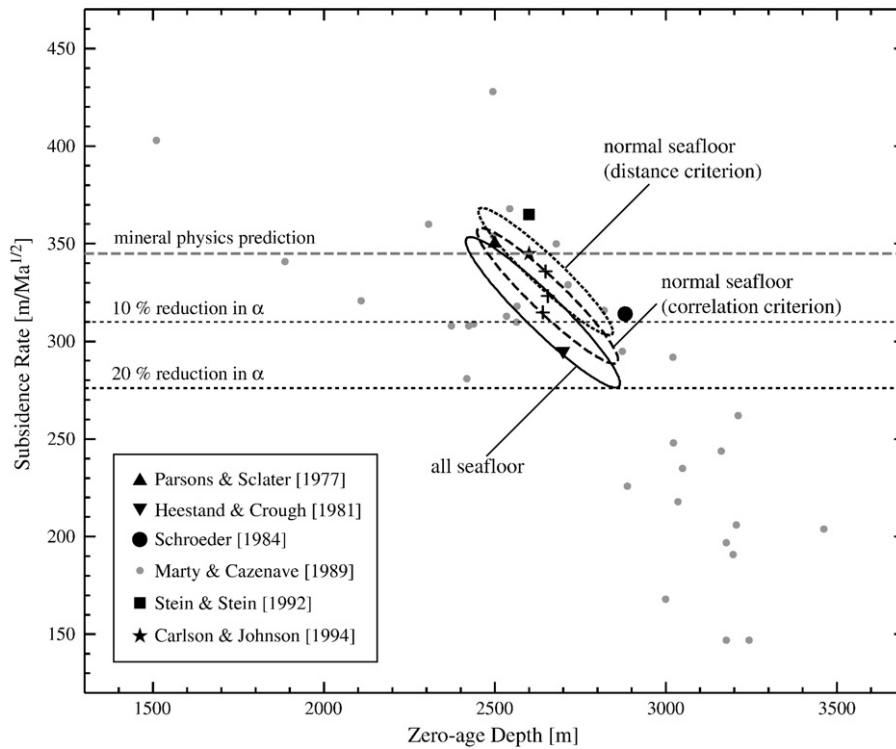


Fig. 6. Summary of estimated subsidence parameters for half-space cooling, from this study (shown as error ellipses, which are the same as shown in Figs. 2c, 5c, and 5d) as well as previous studies (Parsons and Sclater, 1977; Stein and Stein, 1992; Carlson and Johnson, 1994; Marty and Cazenave, 1989; Heestand and Crough, 1981; Schroeder, 1984). Note that Marty and Cazenave (1989) divided ocean basins into 32 tectonic provinces, and the subsidence rate was estimated for these individual provinces. Dashed horizontal line denotes the prediction of half-space cooling with temperature-dependent mantle properties ($345 \text{ m Ma}^{-1/2}$), and dotted lines indicate the influence of 10% and 20% reduction in effective thermal expansivity.

where α is volumetric thermal expansivity, ΔT is the difference between the surface temperature and the initial mantle temperature, κ is thermal diffusivity, ρ_m is mantle density, and ρ_w is water density. By using commonly used values, $\alpha = 3 \times 10^{-5} \text{ K}^{-1}$, $\Delta T = 1350 \text{ K}$, $\kappa = 10^{-6} \text{ m}^2 \text{ s}^{-1}$, $\rho_m = 3300 \text{ kg m}^{-3}$, and $\rho_w = 1000 \text{ kg m}^{-3}$, we obtain $b \sim 370 \text{ m Ma}^{-1/2}$.

Some of mantle properties are, however, known to be strongly temperature-dependent, and the above relation is only an approximation. In order to obtain a more precise prediction for the subsidence rate, we need to solve the following equation of heat conduction:

$$\rho(T)C_P(T)\frac{\partial T}{\partial t} = \frac{\partial}{\partial z}\left(k(T)\frac{\partial T}{\partial z}\right), \quad (3)$$

where C_P and k denote specific heat and thermal conductivity, respectively. The temperature-dependency of density is controlled by thermal expansivity as

$$\rho(T) = \rho_0 \exp\left(-\int_{T_0}^T \alpha(T)dT\right), \quad (4)$$

where ρ_0 is reference density at $T = T_0$. Pressure dependency is not important for lithospheric depth scales (Doyn and Fleitout, 1996), so it is ignored here. Temperature effects are significant; for a temperature variation expected within lithosphere ($\sim 1300 \text{ K}$), α increases by $\sim 30\%$ (Bouhfid et al., 1996), C_P increases by $\sim 60\%$ (Berman and Aranovich, 1996), and k

decreases by $\sim 50\%$ (Hofmeister, 1999). This equation was solved numerically with finite-difference approximation, for a uniformly hot mantle ($T = 1623 \text{ K}$) at $t = 0$ subject to instantaneous cooling with the surface temperature of 273 K . We limit the depth extent of our computation to 300 km . Seafloor subsidence can then be calculated by

$$w(t) = \frac{1}{\rho_i - \rho_w} \left\{ \int_0^\infty [\rho(T(0, z)) - \rho(T(t, z))] dz \right\}, \quad (5)$$

where ρ_i is the average density of the initial mantle column. Even with the variable material properties, seafloor subsidence still follows closely the \sqrt{t} behavior, with the rate of $\sim 345 \text{ m Ma}^{-1/2}$. Surface heat flow can be calculated as $q(t) = k \partial T(t, z) / \partial z|_{z=0}$, and the numerical solution is best approximated by $q = 550 / \sqrt{t}$ (cf. Lister, 1977), where q is in mW m^{-2} and t in Ma .

Thus, the average subsidence rate of $\sim 320 \text{ m Ma}^{-1/2}$ seems to be a bit too low given the currently available mineral physics data, though it is still marginally comparable if uncertainty is taken into account (Fig. 6). One may attempt to explain the low subsidence rate by reducing ΔT , but then, the potential temperature of suboceanic mantle has to be reduced to $1250 \text{ }^\circ\text{C}$, which is $\sim 100 \text{ K}$ lower than what the petrology of mid-ocean ridge basalts indicates for the average ambient mantle (Klein and Langmuir, 1987; Herzberg et al., 2007).

On the other hand, it is recently proposed that the effective thermal expansivity for lithosphere as a whole may be systematically lower than mineral physics data by $\sim 10\text{--}20\%$ (Korenaga,

2007a). The evolution of oceanic lithosphere is characterized by rapid cooling with a large temperature contrast, and because mantle viscosity is strongly temperature-dependent, oceanic lithosphere may not be able to attain complete thermal contraction, which requires efficient viscous relaxation. If the viscoelastic analysis of an evolving oceanic lithosphere (Korenaga, 2007a) is correct, therefore, the subsidence rate could be reduced by $\sim 10\text{--}20\%$, which is comparable with what our global analysis suggests (Fig. 6). The reduced thermal expansivity, if real, has profound implications for the rheological structure of oceanic lithosphere as well as the generation of plate tectonics (Korenaga, 2007a,b).

4.2. The origin of seafloor 'flattening'

Simple half-space cooling has traditionally been thought to be invalid for seafloor older than $\sim 70\text{--}80$ Ma. There are mainly two views for why half-space cooling is not applicable for older seafloor. Proponents for the plate model, which limits the growth of oceanic lithosphere by imposing a temperature boundary condition (Parsons and Sclater, 1977; Stein and Stein, 1992; McKenzie, 1967), claim that oceanic lithosphere has its intrinsic thickness, which may be regulated by convective instability, background heat supply, or some other undefined sources. Others suggest that seafloor flattening is a natural consequence of another well-known aging effect besides cooling (Smith and Sandwell, 1997; Schroeder, 1984; Davies, 1988; Heestand and Crough, 1981); seafloor topography is substantially affected by the formation of oceanic islands and plateaus, and older seafloor is more likely to have encountered these anomalous events.

Our global analysis may support the latter view. We estimated the subsidence parameters for the normal seafloor younger than 70 Ma by assuming half-space cooling, and its prediction for older ages is also shown in Fig. 5a,b. The uncertainty of zero-age depth and subsidence rate (i.e., 68% confidence zone) as well as one standard deviation of prediction error are taken into account when drawing the upper and lower bounds, so age–depth data falling

within these bounds can be considered as consistent with half-space cooling. Thus, the normal seafloor following half-space cooling does exist for almost all ages, which may be seen more clearly in the area–age distribution (Fig. 7). This has been repeatedly suggested in the past (Marty and Cazenave, 1989; Heestand and Crough, 1981), but tends to be overlooked probably due to the popularity of the plate model.

We note that data exceeding the upper bound also exist at older seafloor, so even if we filter out perturbed seafloor by the correlation criterion or by the distance criterion, the signal of seafloor flattening is still present. The significance of such signal is, however, uncertain. As previously mentioned, there is less seafloor at older ages because of subduction, and within the surviving seafloor, the fraction of the normal seafloor is expected to decrease with time, because older seafloor is more likely to be affected, either directly or indirectly, by the emplacement of anomalous crust. Both definitions of the perturbed seafloor are consistent in showing that the majority of the so-called seafloor flattening at old ages is caused by the emplacement of the anomalous crust, and the remaining flattening is supported by only a small fraction of global data (Fig. 7). Our screening criteria are unlikely to be perfect. The detail of the remaining signal is sensitive to how exactly we define the perturbed seafloor, and thus it appears as a second-order feature of global age–depth data, questioning the need for any global mechanism for seafloor 'flattening' (Parsons and McKenzie, 1978; Huang and Zhong, 2005; Davis, 1989; Humler et al., 1999).

Besides depth data, half-space cooling has sometimes been considered inadequate (Stein and Stein, 1992) because its prediction for heat flow may be seen as systematically lower than the observed (Fig. 8a). Heat flow data are considerably more scattered than depth data, and one may question if they can ever distinguish between different cooling models (Carlson and Johnson, 1994). Though we also think that heat flow data are not particularly diagnostic, we would like to point out that the heat flow prediction by half-space cooling is actually very similar to that by the plate model, if half-space cooling is

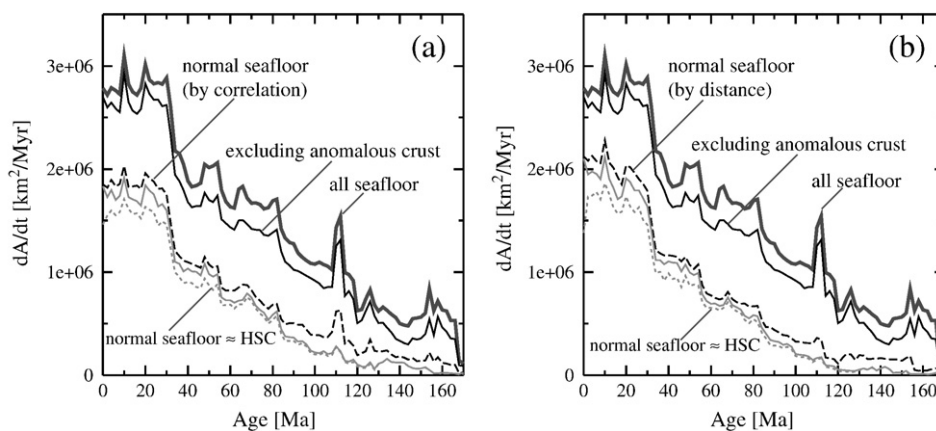


Fig. 7. (a) Area–age distribution of seafloor. Thick solid curve is for all seafloor with known age and with sediment thickness less than 2 km. Thin solid curve shows the result of excluding the anomalous crust. Dashed curve is for the normal seafloor according to the correlation criterion, and dotted curve is for the normal seafloor that is consistent with half-space cooling. The region bounded by dashed curve and gray curve denotes the area of seafloor shallower than the upper bound of half-space cooling prediction (i.e., the upper curve in Fig. 5a) and the region bounded by gray and dotted curves denotes the area of seafloor deeper than the lower bound. (b) Same as (a) but for the distance criterion.

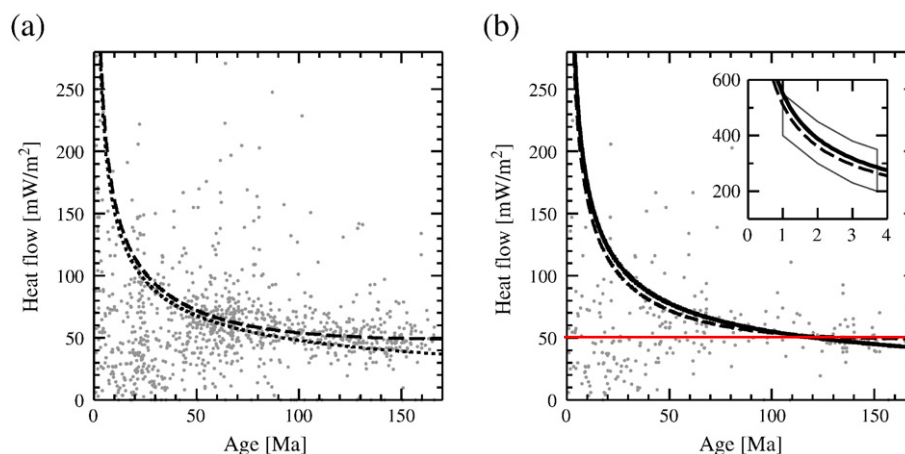


Fig. 8. (a) Age-heat flow relation. Grey dots shows all of available heat flow data (International Heat Flow Commission of IASPEI, 2006) for seafloor with known age. Predictions by the plate model (Stein and Stein, 1992) and the traditional half-space cooling model (Carlson and Johnson, 1994) are shown by dashed and dotted curves, respectively. (b) Same as (a) but for the normal seafloor according to the correlation criterion. Solid curve corresponds to half-space cooling with temperature-dependent mantle properties ($q=550/\sqrt{t}$), and dashed curve to the plate model (Stein and Stein, 1992). Inset shows the range of so far the best calibrated heat flow data on very young seafloor (Davis et al., 1999).

modeled with realistic (i.e., temperature-dependent) mantle properties (Fig. 8b). Even if heat flow data are important as suggested by Stein and Stein (1992), therefore, the similarity between these two predictions casts a doubt on the need for the plate model.

4.3. Small-scale convection and the geoid

Our preceding discussion suggests that simple half-space cooling may be sufficient to explain the evolution of the normal seafloor, but this does not necessarily reject the notion of small-scale convection beneath oceanic lithosphere, which has frequently been discussed as a possible cause of seafloor flattening (Parsons and McKenzie, 1978; Huang and Zhong, 2005). Small-scale convection by itself, however, does not slow down seafloor subsidence (O'Connell and Hager, 1980) and hardly affects surface heat flow (Korenaga and Jordan, 2002). In general, the signal of sublithospheric convection is too subtle (if any) in surface observables. Recent surface-wave tomography of the Pacific mantle (Ritzwoller et al., 2004) suggests that old lithosphere does not follow half-space cooling, which may imply the operation of small-scale convection. As such old seafloor in the Pacific is so heavily populated with hotspot chains and plateaus (Fig. 1a,b), however, we probably cannot extract the evolution of normal lithosphere from their tomography given its spatial resolution. Although small-scale convection is unlikely to affect seafloor subsidence, its presence is still physically plausible according to our understanding of mantle rheology (Korenaga and Jordan, 2003). The most likely place for such convective instability would be beneath fracture zones because of lateral temperature gradient imposed by age difference (Huang et al., 2003), which would be efficiently removed once convection takes place. Weak geoid contrasts at fracture zones, sometimes interpreted to support the plate model (Richardson et al., 1995), may thus be due to small-scale convection and do not contradict

with our notion that half-space cooling is sufficient for the normal seafloor at large.

Although the support for the plate model from local geoid anomalies may be disputed as above, a similar argument based on small-scale convection does not apply to the global geoid signal. Indeed, DeLaughter et al. (1999) claim that global correlation between age and geoid slope prefers the plate model, though the following two issues may undermine their argument. First, as the global geoid is dominated by long-wavelength signals from mantle convection, they filtered out the long-wavelength components and focused on the geoid slope in the remaining signal. As Hager (1983) demonstrated, however, isostatic geoid signals predicated from the half-space cooling model and the plate model differ only in long wavelengths. Thus, we do not expect to be able to discriminate between the two models using the filtered geoid. The geoid slope in the filtered data fluctuates around zero, indicating that it does not contain meaningful signals. Second, when they compare this near-zero geoid-slope observation with model predictions, model predictions remain unfiltered. The plate model predicts zero geoid slope at old seafloor (because plate thickness becomes constant) while the half-space cooling model does not. Thus, the plate model appears to be successful (at least for old seafloor) to explain the near-zero geoid-slope observation, but this success is merely an artifact of treating model predictions and observations differently. In any case, extracting weak lithospheric signals from the geoid is not a trivial task, and using it further to constrain a cooling model is controversial at best.

Acknowledgments

This work was sponsored by the U.S. National Science Foundation under grant EAR-0449517. The authors thank Geoff Davies, Editor Claude Jaupart, and an anonymous reviewer for constructive comments.

References

- Berman, R.G., Aranovich, L.Y., 1996. Optimized standard state and solution properties of minerals: 1. model calibration for olivine, orthopyroxene, cordierite, garnet, and ilmenite in the system FeO–MgO–CaO–Al₂O₃–TiO₂–SiO₂. *Contrib. Mineral. Petrol.* 126, 1–24.
- Bouhifd, M.A., Andraut, D., Fiquet, G., Richet, P., 1996. Thermal expansion of forsterite up to the melting point. *Geophys. Res. Lett.* 23, 1143–1146.
- Calmant, S., Berge-Nguyen, M., Cazenave, A., 2002. Global seafloor topography from a least-squares inversion of altimetry-based high-resolution mean sea surface and shipboard soundings. *Geophys. J. Int.* 151, 795–808.
- Carlson, R.L., Johnson, H.P., 1994. On modeling the thermal evolution of the oceanic upper mantle: An assessment of the cooling plate model. *J. Geophys. Res.* 99, 3201–3214.
- Coffin, M.F., Eldholm, O., 1994. Large igneous provinces: crustal structure, dimensions, and external consequences. *Rev. Geophys.* 32, 1–36.
- Crosby, A.G., McKenzie, D., Sclater, J.G., 2006. The relationship between depth, age and gravity in the oceans. *Geophys. J. Int.* 166, 443–573.
- Davies, G.F., 1988. Ocean bathymetry and mantle convection: 1. large-scale flow and hotspots. *J. Geophys. Res.* 93, 10467–10480.
- Davis, E.E., 1989. Thermal aging of oceanic lithosphere. In: Wright, J.A., Loudon, K.E. (Eds.), *Handbook of Seafloor Heat Flow*. CRC Press, Boca Raton, FL, pp. 145–167.
- Davis, E.E., Chapman, D.S., Wang, K., Villinger, H., Fisher, A.T., Robinson, S.W., Grigel, J., Pribnow, D., Stein, J., Becker, K., 1999. Regional heat flow variations across the sedimented Juan de Fuca Ridge eastern flank: constraints on lithospheric cooling and lateral hydrothermal heat transport. *J. Geophys. Res.* 104, 17675–17688.
- DeLaughter, J., Stein, S., Stein, C.A., 1999. Extraction of a lithospheric cooling signal from oceanwide geoid data. *Earth Planet. Sci. Lett.* 174, 173–181.
- Divins, D.L., NGDC total sediment thickness of the world's oceans and marginal seas, 2006/07/11 <http://www.ngdc.noaa.gov/mgg/sedthick/sedthick.html>.
- Doin, M.P., Fleitout, L., 1996. Thermal evolution of the oceanic lithosphere: an alternative view. *Earth Planet. Sci. Lett.* 142, 121–136.
- Efron, B., 1982. *The jackknife, the bootstrap, and other resampling plans*. SIAM, Philadelphia, PA.
- Hager, B.H., 1983. Global isostatic geoid anomalies for plate and boundary layer models of the lithosphere. *Earth Planet. Sci. Lett.* 63, 97–109.
- Heestand, R.L., Crough, S.T., 1981. The effect of hot spots on the oceanic age–depth relation. *J. Geophys. Res.* 86, 6107–6114.
- Herzberg, C., Asimow, P.D., Arndt, N., Niu, Y., Leshner, C.M., Fitton, J.G., Cheadle, M.J., Saunders, A.D., 2007. Temperatures in ambient mantle and plumes: constraints from basalts, picrites, and komatiites. *Geochem. Geophys. Geosys.* 8 (2), Q02206. doi:10.1029/2006GC001390.
- Hillier, J.K., Watts, A.B., 2005. Relationship between depth and age in the North Pacific ocean. *J. Geophys. Res.* 110, B02405. doi:10.1029/2004JB003406.
- Hofmeister, A.M., 1999. Mantle values of thermal conductivity and the geotherm from phonon lifetimes. *Science* 283, 1699–1706.
- Huang, J., Zhong, S., 2005. Sublithospheric small-scale convection and its implications for residual topography at old ocean basins and the plate model. *J. Geophys. Res.* 110, B05404. doi:10.1029/2004JB003153.
- Huang, J., Zhong, S., van Hunen, J., 2003. Controls on sublithospheric small-scale convection. *J. Geophys. Res.* 108 (B8), 2405. doi:10.1029/2003JB002456.
- Humler, E., Langmuir, C., Daux, V., 1999. Depth versus age: new perspective from the chemical compositions of ancient crust. *Earth Planet. Sci. Lett.* 173, 7–23.
- International Heat Flow Commission of IASPEI. Global heat flow database, 2006/05/11, <http://www.heatflow.und.edu/index2.html>.
- Kido, M., Seno, T., 1994. Dynamic topography compared with residual depth anomalies in oceans and implications for age–depth curves. *Geophys. Res. Lett.* 21, 717–720.
- Klein, E.M., Langmuir, C.H., 1987. Global correlations of ocean ridge basalt chemistry with axial depth and crustal thickness. *J. Geophys. Res.* 92, 8089–8115.
- Korenaga, J., 2007a. Effective thermal expansivity of Maxwellian oceanic lithosphere. *Earth Planet. Sci. Lett.* 257, 343–349. doi:10.1016/j.epsl.2007.03.010.
- Korenaga, J., 2007b. Thermal cracking and the deep hydration of oceanic lithosphere: a key to the generation of plate tectonics? *J. Geophys. Res.* 112, B05408. doi:10.1029/2006JB004502.
- Korenaga, J., Jordan, T.H., 2002. On 'steady-state' heat flow and the rheology of oceanic mantle. *Geophys. Res. Lett.* 29, 2056. doi:10.1029/2002GL016085.
- Korenaga, J., Jordan, T.H., 2003. Physics of multiscale convection in Earth's mantle: Onset of sub-lithospheric convection. *J. Geophys. Res.* 108 (B7), 2333. doi:10.1029/2002JB001760.
- Lister, C.R.B., 1977. Estimators for heat flow and deep rock properties based on boundary layer theory. *Tectonophysics* 41, 157–171.
- Marty, J.C., Cazenave, A., 1989. Regional variations in subsidence rate of oceanic plates: a global analysis. *Earth Planet. Sci. Lett.* 94, 301–315.
- McKenzie, D.P., 1967. Some remarks on heat flow and gravity anomalies. *J. Geophys. Res.* 72, 6261–6273.
- Moser, T.J., 1991. Shortest path calculation of seismic rays. *Geophysics* 56, 59–67.
- Müller, R.D., Roest, W.R., Royer, J.-Y., Gahagan, L.M., Sclater, J.G., 1997. Digital isochrons of the world's ocean floor. *J. Geophys. Res.* 102, 3211–3214.
- O'Connell, R.J., Hager, B.H., 1980. On the thermal state of the earth. In: Dziewonski, A.M., Boschi, E. (Eds.), *Physics of the Earth's Interior*. Proc. Int. Sch. Phys., vol. 78. Enrico Fermi, Amsterdam, pp. 270–317.
- Parsons, B., 1982. Causes and consequences of the relation between area and age of the ocean floor. *J. Geophys. Res.* 87, 289–302.
- Parsons, B., Sclater, J.G., 1977. An analysis of the variation of ocean floor bathymetry and heat flow with age. *J. Geophys. Res.* 82, 803–827.
- Parsons, B., McKenzie, D., 1978. Mantle convection and the thermal structure of the plates. *J. Geophys. Res.* 83, 4485–4496.
- Phipps Morgan, J., Morgan, W.J., Price, E., 1995. Hotspot melting generates both hotspot volcanism and a hotspot swell? *J. Geophys. Res.* 100, 8045–8062.
- Renkin, M.L., Sclater, J.G., 1988. Depth and age in the North Pacific. *J. Geophys. Res.* 93, 2919–2935.
- Ribe, N.M., Christensen, U.R., 1994. Three-dimensional modeling of plume–lithosphere interaction. *J. Geophys. Res.* 99, 669–682.
- Richardson, W.P., Stein, S., Stein, C.A., Zuber, M.T., 1995. Geoid data and thermal structure of the oceanic lithosphere. *Geophys. Res. Lett.* 22, 1913–1916.
- Ritzwoller, M.H., Shapiro, N.M., Zhong, S., 2004. Cooling history of the Pacific lithosphere. *Earth Planet. Sci. Lett.* 226, 69–84.
- Schroeder, W., 1984. The empirical age–depth relation and depth anomalies in the Pacific ocean basin. *J. Geophys. Res.* 89, 9873–9883.
- Sclater, J.G., Wixon, L., 1986. The relationship between depth and age and heat flow and age in the western North Atlantic. In: Vogt, P.R., Tucholke, B.E. (Eds.), *The Western Atlantic Region*, vol. M, *Geology of North America*. Geological Society of America, Boulder, CO, pp. 257–270.
- Smith, W.H., Sandwell, D.T., 1997. Global sea floor topography from satellite altimetry and ship depth soundings. *Science* 277, 1956–1962.
- Stein, C.A., Stein, S., 1992. A model for the global variation in oceanic depth and heat flow with lithospheric age. *Nature* 359, 123–129.
- Stein, C.A., Stein, S., 1993. Constraints on Pacific midplate swells from global depth–age and heat flow–age models. *The Mesozoic Pacific: Geology, Tectonics, and Volcanism*. American Geophysical Union, Washington, D.C., pp. 53–76.
- Turcotte, D.L., Schubert, G., 1982. *Geodynamics: Applications of continuum physics to geological problems*. John Wiley and Sons, New York.
- White, R.S., McKenzie, D., O'Nions, R.K., 1992. Oceanic crustal thickness from seismic measurements and rare earth element inversions. *J. Geophys. Res.* 97, 19683–19715.